Theory of Optical Transmission through Elliptical Nanohole Arrays

Yakov M. Strelniker*
Department of Physics, Bar-Ilan University, 52900 Ramat-Gan, Israel
(Dated: February 6, 2008)

We present a theory which explains (in the quasistatic limit) the experimentally observed [R. Gordon, *et al*, Phys. Rev. Lett. **92**, 037401 (2004)] squared dependence of the depolarization ratio on the aspect ratio of the holes, as well as other features of extraordinary light transition. We calculated the effective dielectric tensor of a metal film penetrated by elliptical cylindrical holes and found the extraordinarily light transmission at special frequencies related to the surface plasmon resonances of the composite film. We also propose to use the magnetic field for getting a strong polarization effect, which depends on the ratio of the cyclotron to plasmon frequencies.

PACS numbers: 64.60.Ak, 73.23.-b; 72.80.Tm, 78.66.Sq, 77.84.Lf

A pioneering article of Ebbesen *et. al*[1] reported on an extraordinary optical transmission through periodic holes array in metallic films. This was explained by the coupling of light with surface plasmons. In most of the articles[2] published after Ref. 1, the surface plasmons were treated as the coupled waves, propagating along both film surfaces (in framework of the theory described in Ref. 3). In this approach the periodicity and spacing between the holes were taken into account, but the shape of the holes was not. In Ref. 4 it was even written that in "the long-wavelength limit ... the transmission coefficient ... does not appreciably depend on hole-shape". In contrast to this, in our paper 5 we treat the plasmon as the excitations localized around the holes[6]. It was shown that the present of the magnetic field transforms the initially circular holes into elliptical ones in the rescaled virtual coordinate space. That is, it was predicted that the elliptical shape of inclusions should induce some anisotropy into the system. This prediction was apparently not known to the authors of Ref. 7, who actually confirmed it in their recent experiment on light transmission through a periodical array of real (not virtual) *elliptical holes*.

In this paper we present a theory, which in the quasistatic (long wavelength) limit explains the squared dependence of the depolarization ratio on the aspect ratio of the holes (experimentally observed in Ref. 7), as well as other optical features. This theory is a further development of our methods described in Refs. 5,8,9. We also note that similar effects (e.g., light polarization) can be reached by applying a static magnetic field.

Let us consider a geometry which corresponds to the above-mentioned experiment[7]: a metal film with a square array of identical perpendicular elliptical holes. A monochromatic light beam of angular frequency ω impinges upon this film along the perpendicular axis y, with linear polarization along the principal axis x of the array (see Fig. 1).

Following Refs. 5,8,9, we can treat the holes as dielectric inclusions embedded in a conducting host.[5,10] In this

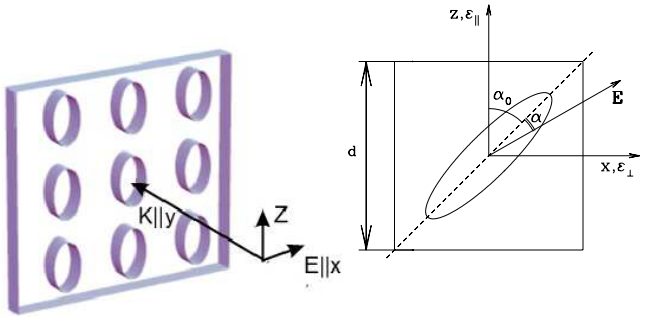

(a) (b)

FIG. 1: (a) A schematic drawing of a metal film with a periodic array of elliptical holes. The incident light beam is normal to the film surface, i.e., the *ac* electric field **E** is parallel to the film plane, while the wave vector is normal to it (i.e., $\mathbf{k} \parallel y$). (b) An elliptical hole in a unit cell when the main semi-axes a and c are inclined in respect to the lattice axes x and z by an angle α_0.

approach, the local electric potential $\phi^{(\alpha)}(\mathbf{r})$ is then the solution of a boundary value problem based upon the Laplace partial differential equation

$$\nabla \cdot \hat{\varepsilon}_M \cdot \nabla \phi^{(\alpha)} = \nabla \cdot \theta_I \delta\hat{\varepsilon} \cdot \nabla \phi^{(\alpha)}, \qquad (1)$$

and the boundary condition $\phi^{(\alpha)} = r_\alpha$. Here r_α is the α-component of $\mathbf{r}$, $\hat{\varepsilon}_I$ and $\hat{\varepsilon}_M$ are the electrical permittivity tensors of the *inclusions* and the *metal* host respectively, $\delta\hat{\varepsilon} \equiv \hat{\varepsilon}_M - \hat{\varepsilon}_I$, $\theta_I(\mathbf{r})$ is the characteristic function describing the location and the shape of the inclusions ($\theta_I = 1$ inside the inclusions and $\theta_I = 0$ outside of them).[5,10,11]

The host with the anisotropic permittivity tensor $\hat{\varepsilon}_M$ can be transformed to an isotropic $\hat{\varepsilon}'_M$ using the rescaling of the Cartesian coordinates ($\xi_1 \equiv x/\sqrt{\varepsilon_{xx}}$, $\xi_2 \equiv y/\sqrt{\varepsilon_{yy}}$, $\xi_3 \equiv z/\sqrt{\varepsilon_{zz}}$). Then elliptic cylinder inclusion will be transformed into some new elliptic cylinder in the rescaled virtual ξ-space, and the electric field $\mathbf{E}_I = \nabla\phi_I$ inside this single inclusion {inclined by some angle α_0 in respect to the main axes [see Fig. 1(b)]} can be found from the system of linear equations[12,13]

$$E^{(I)}_\alpha = E_{0\alpha} + \sum_{\beta,\gamma} n_{\alpha\beta}\delta\varepsilon_{\beta\gamma}(\varepsilon^{(M)}_{\alpha\alpha}\varepsilon^{(M)}_{\beta\beta})^{-1/2}E^{(I)}_\gamma, \qquad (2)$$

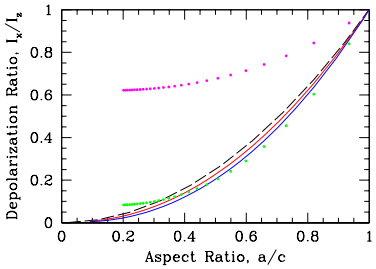

FIG. 2: (Color online) The depolarization ratio of the transmitted light as a function of the aspect ratio a/c of the holes for different λ. For the values of λ from ~ 900 nm to ~ 700 nm the curves are close enough to the square law $y = x^2$ (left dashed curve), while already for $\lambda = 550$ nm and $\lambda = 500$ nm (shown by dotted lines) the polarization ratio is essentially different from this law.

where $n_{\alpha\beta}$ are the Cartesian components of the depolarization factor[12,13]. The latter can be transformed to the diagonal form $n_{\alpha\beta} = n_\alpha \delta_{\alpha\beta}$ by a simple coordinate rotation $\mathbf{r}' = \hat{R}(\alpha_0)\cdot\mathbf{r}$, where α_0 is the angle on inclination of the elliptical holes from the lattice axes [see Fig. 1(b)], $\hat{R}(\alpha_0)$ is the rotation matrix

$$\hat{R}(\alpha_0) = \{(\cos\alpha_0, -\sin\alpha_0), (\sin\alpha_0, \cos\alpha_0)\}, \quad (3)$$

which directs the new coordinate axes along the principal ellipse axes. Note that $n_{\alpha\beta}$ (as well as n_α) now depends on the precise shape of the transformed inclusion, and therefore is a function of $\hat{\varepsilon}_M$. If the coordinate axes are the principal axes of the inclusion ($n_{\alpha\beta} = n_\alpha \delta_{\alpha\beta}$), then the elliptic cylindric hole of the semi-axes a and c (with symmetry axis along y) transforms in ξ-space into a new elliptic cylinder with semi-axes $a' = a/\sqrt{\varepsilon_{xx}}$ and $c' = c/\sqrt{\varepsilon_{zz}}$ for which:

$$n_x = \frac{c'}{a'+c'} = \frac{c\sqrt{\varepsilon_{xx}}}{c\sqrt{\varepsilon_{xx}} + a\sqrt{\varepsilon_{zz}}}, \quad (4)$$

$$n_y = 0, \quad n_z = 1 - n_x, \quad (5)$$

For simplicity, we assume the host permittivity tensor has the form $\hat{\varepsilon} = \varepsilon_0 \cdot \hat{I} + i\frac{4\pi}{\omega}\hat{\sigma}$, where the conductivity tensor $\hat{\sigma}$ is taken in the free-electron Drude approximation with $\mathbf{B}_0 \parallel z$:

$$\hat{\sigma} = \frac{\omega_p^2 \tau}{4\pi} \begin{pmatrix} \frac{1-i\omega\tau}{(1-i\omega\tau)^2+H^2} & \frac{-H}{(1-i\omega\tau)^2+H^2} & 0 \\ \frac{H}{(1-i\omega\tau)^2+H^2} & \frac{1-i\omega\tau}{(1-i\omega\tau)^2+H^2} & 0 \\ 0 & 0 & \frac{1}{1-i\omega\tau} \end{pmatrix}, \quad (6)$$

ε_0 is the scalar dielectric constant of the background ionic lattice, and $\hat{I}$ is the unit tensor. The magnetic field enters only through the Hall-to-Ohmic resistivity ratio $H \equiv \rho_H/\rho = \sigma_{xy}/\sigma_{xx} = \mu|\mathbf{B}_0| = \omega_c\tau$, where $\omega_c = eB/mc$ is the cyclotron frequency, τ is the conductivity relaxation time, $\omega_p = \left(4\pi e^2 N_0/m\right)^{1/2}$ is the plasma frequency, N_0 is the charge carrier concentration, m is its effective mass, and μ is the Hall mobility.

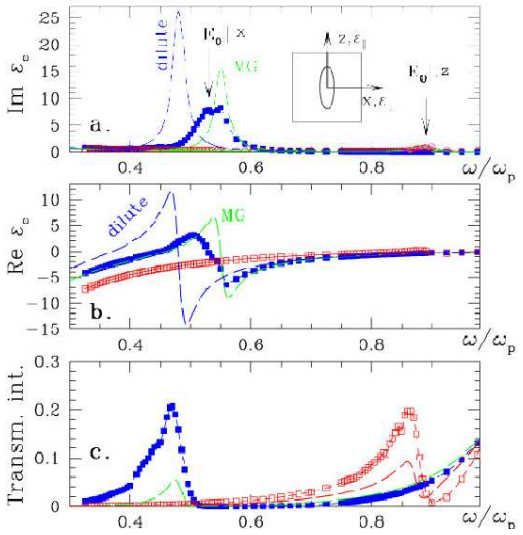

FIG. 3: (Color online) Transmission spectrum through an elliptical nanohole arrays for the p- and s- linear light polarizations. The p polarization is parallel to the [0,1] direction, while s is parallel to the [1,0] direction. (a) $Im\ \varepsilon_{xx}^{(e)}$ ($\mathbf{E_0} \parallel x$, p polarization) and $Im\ \varepsilon_{zz}^{(e)}$ ($\mathbf{E_0} \parallel z$, s-polarization) vs. ω/ω_p. (b) Re $\varepsilon_{xx}^{(e)}$ and Re $\varepsilon_{zz}^{(e)}$ vs. ω/ω_p. In both polarizations there is an SP resonance peak at $\omega = \omega_{sp\,x}$ and $\omega = \omega_{sp\,z}$ (shown by the arrow), respectively. When $\mathbf{E_0} \parallel z$, the resonance shifts for larger values ($\omega_{sp\,z} > \omega_{sp\,x}$) and its amplitude reduces drastically. (c) Transmission coefficient T vs. frequency ω, for different polarizations $\mathbf{E} \parallel x$ and $\mathbf{E} \parallel z$. The analytical results obtained using a dilute and MG approximations are indicated by dashed curves. The (connected by lines) filled and open symbols denote the results obtained numerically[10] for a square array of holes in the shape of elliptical cylinders. Inset to Fig. (a): a unit cell with the elliptic hole and coordinate axes.

When $\varepsilon_{xx} = \varepsilon_{zz}$ ($H = 0$), we have $n_x = c/(a+c)$, $n_z = a/(a+c)$. However, when $H > 0$ the depolarization factor has a complicated dependence on ω.

Solving the system of linear equations (2), we obtain the following expression for the uniform electric field inside the original elliptical cylinder (when $\mathbf{B}_0 \parallel z$):

$$\mathbf{E}_I = \hat{\gamma} \cdot \mathbf{E_0}, \quad (7)$$

where $\hat{\gamma}$ is a 3×3 matrix whose nonzero components are: $\gamma_{xx} = \varepsilon_{xx}/(\varepsilon_{xx} - n_x\delta\varepsilon_{xx})$, $\gamma_{xy} = n_x\delta\varepsilon_{xy}/(\varepsilon_{xx} - n_x\delta\varepsilon_{xx})$, $\gamma_{yy} = 1$, $\gamma_{zz} = \varepsilon_{zz}/(\varepsilon_{zz} - n_z\delta\varepsilon_{zz})$.

From Eq. (7) it follows that the depolarization ratio [i.e., the ratio of the light intensity I_x (polarized parallel to x-axis) to the light intensity I_z (polarized parallel to z-axis), and therefore proportional to $|E_x/E_z|^2$], can be written (in the case of $n_{\alpha\beta} = n_\alpha\delta_{\alpha\beta}$) as

$$\frac{I_x}{I_z} = \left| \sqrt{\frac{\varepsilon_{xx}^{(M)}}{\varepsilon_{zz}^{(M)}}} \left(\frac{c\sqrt{\varepsilon_{zz}^{(M)}\varepsilon_{xx}^{(M)}} + a\varepsilon_{zz}^{(I)}}{a\sqrt{\varepsilon_{zz}^{(M)}\varepsilon_{xx}^{(M)}} + c\varepsilon_{xx}^{(I)}} \right) \left(\frac{E_{0\,x}^{(I)}}{E_{0\,z}^{(I)}} \right) \right|^2. \quad (8)$$

Let us consider the case of zero magnetic field, $H = 0$, when both the host and the inclusions are isotropic and, therefore, are characterized by the scalar tensors $\hat{\varepsilon}_M = \varepsilon_M \cdot \hat{I}$, $\hat{\varepsilon}_I = \varepsilon_I \cdot \hat{I}$ (where $\hat{I}$ is a unit matrix). We assume also that $E_{0\,x} = E_{0\,z}$. When $c\varepsilon_M \gg a\varepsilon_I$ and $a\varepsilon_M \gg c\varepsilon_I$, what might be true in the simple limit $\varepsilon_0 \ll \sigma/\omega$ and $\omega\tau \gg 1$ with $H = 0$ (situation of Ref. 7), then from Eq. (8) it follows that

$$I_x/I_z \;=\; |E_x^{(I)}/E_z^{(I)}|^2 \simeq (c/a)^2, \qquad (9)$$

as in Fig. 4 of Ref. 7.

In Fig. 2 we show the ratio (8) for different wavelengths, λ. Using the data[15] of the complex permittivity ε_M of the evaporated gold, we can see that in the wavelength's range between $\lambda \sim 900$ nm ($\varepsilon_M \sim -28.0 + i1.8$) and $\lambda \sim 700$ nm ($\varepsilon_M \sim -14.7 + i1.0$), the curves are close enough to the law $(c/a)^2$, while already for $\lambda = 500$ nm (for which $\varepsilon_M \sim -3.4 + i0.7$), the polarization ratio $|E_x/E_z|^2$ (shown by the dotted line) is essentially different from this law.

If $H \neq 0$ and $a = c$, then $I_x/I_z = |\varepsilon_{xx}/\varepsilon_{yy}|$ (see Eq. 8). In Drude approximation (6) (and in the limit $\varepsilon_0 \to 0$, $\omega_p\tau \to 1$) this takes the simplest form

$$I_x/I_z = |E_x/E_z|^2 \;=\; \left[1 - (\omega_c/\omega)^2\right]^{-1}, \qquad (10)$$

from which it follows that the depolarization ratio I_x/I_z can be made arbitrarily large, since the value $\omega_c/\omega = (\omega_c/\omega_p)(\omega/\omega_p)^{-1} = (H/\omega_p\tau)(\omega/\omega_p)^{-1}$ [where $H \equiv \omega_c\tau$, see comments to Eq. (6)], can be made as close to 1 as necessary.

Next, we approximately compute the tensor $\hat{\varepsilon}_e(\omega)$, which is defined by the relation $\hat{\varepsilon}_e \cdot \langle \mathbf{E}(\mathbf{r})\rangle = \langle \hat{\varepsilon}(\mathbf{r}) \cdot \mathbf{E}(\mathbf{r})\rangle$, where $\langle ...\rangle$ denotes a volume average, and $\hat{\varepsilon}(\mathbf{r})$ is the local dielectric tensor. In the case of the dilute collection of the elliptic cylinders, the tensor $\hat{\varepsilon}_e$ takes the form[5,10,11] $\hat{\varepsilon}_e = \hat{\varepsilon}_M - p\delta\hat{\varepsilon} \cdot \hat{\gamma}$, where p is the volume fraction of inclusions. For the case $H = 0$ (and when $\mathbf{E_0}$ and the coordinate axes are directed along the symmetry axes of the ellipse), $\hat{\varepsilon}_e$ takes the form

$$\varepsilon_{ii}^{(e)} = \varepsilon_M \left[1 - p\delta\varepsilon_{ii}/(\varepsilon_M - n_i\delta\varepsilon_{ii})\right], \qquad (11)$$

where n_i is given by Eq. (5), and $i = x,\, y,\, z$.

The frequency $\omega_{sp,i}$ of the surface plasmon (SP) polarized in the i^{th} direction is the one in which $\mathbf{E}$ [see Eq. (7) and Eq. (11)] becomes very large even for a very small applied field. This condition is satisfied when $\varepsilon_{M;ii}(\omega_{sp,i}) - n_i\delta\varepsilon_{ii}(\omega_{sp,i}) = 0$. Substituting Eq. (6) into this, and letting $\omega_p\tau \to \infty$, one obtains

$$\omega_{sp,i} = \omega_p\sqrt{(1 - n_i)/[(1 - n_i) + n_i\varepsilon_i^{(I)}]}. \qquad (12)$$

For $\varepsilon_I = 1$ this simplifies into $\omega_{sp,x} = \omega_p\sqrt{1 - n_x}$.

In Maxwell-Garnett (MG) or Clausius-Mossotti approximation[11], expressions for ε_e and ω_{sp} can be obtained directly from Eqs. (11),(12), obtained in dilute approximation just by formal substitution $n_i \to n_i(1 - p)$.[9]

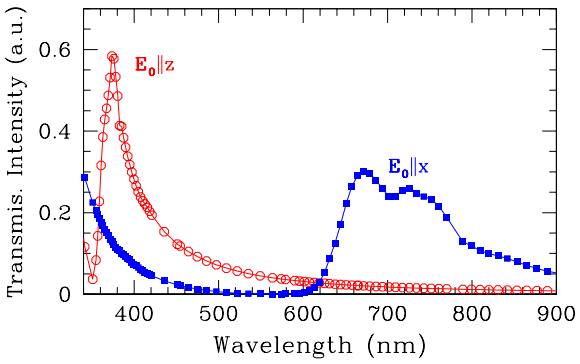

FIG. 4: (Color online) The same as Fig. 3(c), but vs. wavelength λ. The peak at $\lambda \sim 600 - 700$ nm corresponds to $E_0 \parallel x$ (i.e., p-) polarization (shown in Fig. 2 of Ref. 7), while the peak at $\lambda \sim 400$ nm corresponds to $E_0 \parallel x$ polarization (not shown in Fig. 2 of Ref. 7). $\omega_p = 3 \cdot 10^{15}$ rad/s.

When the aspect ratio c/a tends to infinity the considered geometry transforms into the case of the parallel slabs, which can be solved *exactly*: $1/\varepsilon_e = p_M/\varepsilon_M + p_I/\varepsilon_I$. Using the form (6), we can find the resonance frequency $\omega_{sp} = \omega_p\sqrt{p_I/(p_M\varepsilon_I + p_I)}$. This coincides with Eq. (12) in the limit $n_x \to 1$. The other exact solvable geometry, *parallel cylinders*, for which $n_i \to 0$, does not give any resonance: $\varepsilon_e = p_M\varepsilon_M + p_I\varepsilon_I = 1 - p_M(\omega_p/\omega)^2$.

When the cylindrical holes are arranged on a two-dimensional periodic lattice[1,7] a more suitable approach is a Fourier expansion technique[10]. Since $\theta_I(\mathbf{r})$ and $\psi^{(\alpha)} = \phi^{(\alpha)} - r^{(\alpha)}$ are now periodical functions, they can be expanded in a Fourier series. This transforms Eq. (1) into an infinite set of linear algebraic equations for the Fourier coefficients $\psi_{\mathbf{g}}^{(\alpha)} = \frac{1}{V}\int_V \psi^{(\alpha)}(\mathbf{r})e^{-i\mathbf{g}\cdot\mathbf{r}}dV$, where $\mathbf{g} = (2\pi/d)(m_x, m_y, m_z)$ is a vector of the appropriate reciprocal lattice, m_i are the arbitrary integers, d is a lattice constant, and V is the volume of a unit cell. After solving a truncated, finite subset of those equations, we can use those Fourier coefficients $\psi_{\mathbf{g}}^{(\alpha)}$ in order to calculate the bulk effective macroscopic electric permittivity tensor $\hat{\varepsilon}_e$, using the procedure described in Ref. 5,10,11. Note that the Fourier coefficient $\theta_{\mathbf{g}}$ of the $\theta_I(\mathbf{r})$-function of the elliptical hole (inclined by the angle α_0 in respect to the main lattice axes) has the form[5,10] $\theta_{\mathbf{g}} = (4\pi ac/d^3\tilde{g}_\perp)\; J_1(\tilde{g}_\perp)[\sin(|g_z|h/2)/|g_z|]$, where $J_1(x)$ is a Bessel function and $\tilde{g}_\perp(\alpha) = [a^2(g_x\cos\alpha + g_z\sin\alpha)^2 + c^2(g_z\cos\alpha - g_x\sin\alpha)^2]^{1/2}$.

In Figs. 3(a) and 3(b) we show the imaginary and real parts of $\varepsilon_e(\omega)$ vs. ω/ω_p, respectively. The curves without points are the two principal in-plain components $\varepsilon_{xx}^{(e)}$ and $\varepsilon_{zz}^{(e)}$ (corresponding to polarizations $\mathbf{E_0}||x$ and $\mathbf{E_0}||z$, respectively) as obtained in the dilute and MG approximation. The full and open squares in Fig. 3(a) denote the same quantities, but now for a square lattice (of lattice constant d) of elliptical holes with the same aspect ratio and volume fraction p as in MG and dilute approx-

imations. In this case, $\varepsilon_{xx}^{(e)}$ and $\varepsilon_{zz}^{(e)}$ are calculated by the Fourier expansion technique[5] mentioned above.

Finally, in Fig. 3(c), we show the calculated transmission coefficient T for the dielectric functions shown in Figs. 3(a) and 3(b). The dependence of the transmission coefficient T on frequency ω, [as well as on the wave length λ (see Fig. 4)] for different film thicknesses, can be obtained from the effective value ε_e using the known expression[14] for $T = |d|^2$, where $d = (1 - r_{12}^2)/[\exp(-i\chi) - r_{12}^2 \exp(i\chi)]$, and $r_{12} = (1-N)/(1+N)$, $N = \sqrt{\varepsilon_e(\omega)}$, $\chi = (\omega/c)hN = (\omega/\omega_p)(\omega_p h/c)N$, and h is the film thickness.[9] The transmission coefficient $T(\omega)$ [see Fig. 3(c)] shows the characteristic "extraordinary transmission" peaks expected, based on Figs. 3(a),(b). Since the angular dependence of the permittivity tensor in the rotated coordinate system $\hat{\varepsilon}' = \hat{R}(\alpha+\alpha_0)\cdot\hat{\varepsilon}\cdot\hat{R}^{-1}(\alpha+\alpha_0)$ [where $R(\alpha+\alpha_0)$ is given by Eq. (3) and α is the polarization angle i.e., the angle between the vector $\mathbf{E}_0$ and the axes of the ellipse, see Fig. 1(b)] is a cosine-like [e.g., $(\varepsilon_{xx}^{(e)})' = \varepsilon_{xx}^{(e)}\cos^2(\alpha+\alpha_0) + \varepsilon_{zz}^{(e)}\sin^2(\alpha+\alpha_0)$], the angular dependence of the transmission coefficient $T(\alpha)$ looks (depending on the values of a/c and $\omega h/c$) also as a cosine-like. This explains the Malus' law[16] of the light transmission, T, observed in Refs. 7,16.

The amplitudes and frequencies of the peaks (for both polarizations $\mathbf{E_0} \parallel x$ and $\mathbf{E_0} \parallel z$) depend on the aspect-ration a/c. For polarization along z axis the resonance frequency $\omega_{sp\,z}$ shifts for larger value and its amplitude reduces drastically. Estimating the imaginary part of $\delta\varepsilon_{ii}^{(e)} \equiv \varepsilon_{ii}^{(e)} - \varepsilon_M$ [see Eq. (11)] at the resonance frequency $\omega_{sp\,i}$, we found that the ratio Im $\delta\varepsilon_{xx}^{(e)}(\omega_{sp\,x})$/Im $\delta\varepsilon_{zz}^{(e)}(\omega_{sp\,z})$ is of the order $\sim (n_x/n_z)^{5/2} = (c/a)^{5/2}$. For the aspect ratio $a/c = 0.3$ this is of the order ~ 20, in agreement with our numerical calculations [see Fig. 3(a)]. One might expect that in the extraordinary light transition the maximum at $\omega_{sp\,z}$ will also be much smaller when compared to the maximum at $\omega_{sp\,x}$, but [as we can see in Figs. 3(c) and 4], they are of the same order. In Fig. 4 we show the data, presented in Fig. 3(c), in terms of wavelength λ. The calculations were performed for the systems with aspect ratio $a/c = 0.3$, volume fraction of holes, $p = 0.031$, $\varepsilon_I = 1$, $\omega_p\tau = 40$, $\omega_p = 3\cdot 10^{15}$ rad/s (a typical for Au value[7], so that $\omega_p h/c = 1$), $\omega_p\tau = 40$, $\xi = \omega_p h/c = 1$, and the film thickness $h = 100nm$.

In summary, we have studied analytically and numerically the extraordinary transmission through perforated metal films with elliptical holes. We have explained analytically the optical features found experimentally and described in Ref. 7. Our numerical results are in good agreement with experimental data. We also propose to use the magnetic field for getting a strong polarization effect, which depends on the ratio ω_c/ω_p. As a material which may be suitable for this purpose the bismuth can be considered, where the low carrier density ($\sim 3\times 10^{17}$ cm^{-1}) can make the carrier cyclotron energies, ω_c, equal to or greater than the plasmon energy, ω_p.[17]

We thankfully acknowledge useful conversations with David J. Bergman and Nilly Madar. This research was supported in part by grants from the Israel Science Foundation, and the KAMEA Fellowship program of the Ministry of Absorption of the State of Israel.

* Electronic address: strelnik@mail.biu.ac.il

1. T.W. Ebbesen, H. J. Lezec, H. F. Ghaemi, T. Thio, and P. A.Wolff, Nature (London) **391**, 667 (1998).
2. A. Garcia-Martin, G. Armelles, and S. Pereira, Phys. Rev. B **71**, 205116 (2005), and references therein.
3. H. Raether, *Surface Plasmons* (Springer-Verlag, Berlin, 1988).
4. L. Martin-Moreno, *et al*, Phys. Rev. Lett. **86**, 1114 (1998).
5. Y. M. Strelniker and D. J. Bergman, Phys. Rev. B **59**, R12763 (1999).
6. The experimental observation of a plasmon localized around a single hole see e.g. in L. Yin *et al*, Appl. Phys. Lett. **85**, 467 (2004), A. Degiron, H. J. Lezec, and N. Yamamoto, and T. W. Ebbesen Opt. Commun. **239**, 61 (2004), C. Genet and T. W. Ebbesen, Nature **445**, 39 (2007), and references therein.
7. R. Gordon, A.G. Brolo, A. McKinnon, A. Rajora, B. Leathem, and K. L. Kavanagh, Phys. Rev. Lett. **92**, 037401 (2004).
8. D. J. Bergman and Y. M. Strelniker, Phys. Rev. Lett. **80**, 857 (1998); Y. M. Strelniker and D. J. Bergman, Eur. Phys. J. AP **7**, 19 (1999). D. J. Bergman and Y. M. Strelniker, Physica B **279**, 1 (2000).
9. Y. M. Strelniker, D. Stroud, and A. O. Voznesenskaya, Eur. Phys. J. B **52**, 1 (2006); J. Appl. Phys. **99**, 08H702 (2006).
10. Y. M. Strelniker and D. J. Bergman, Phys. Rev. B **50**, 14001 (1994); D. J. Bergman and Y. M. Strelniker, Phys. Rev. B **49**, 16256 (1994).
11. D. J. Bergman and D. Stroud, Solid State Physics **45**, 147 (1992); G. W. Milton, in *The Theory of Composites* (Cambridge, 2002).
12. D. J. Bergman and Y. M. Strelniker, Phys. Rev. B **60**, 13016 (1999).
13. D. J. Bergman and Y. M. Strelniker, Phys. Rev. B **59**, 2180 (1999).
14. L. D. Landau, E. M. Lifshitz, and L. P. Pitaevskii, *Electrodynamics of Continuous Media* (Pergamon Press, Oxford, 1984).
15. G. Hass, L. Hadley, *Optical Properties of Metals*, pp. 6-133, in *American Institute of Physics Handbook*, Third Edition, New York, by ed. D. E. Gray.
16. J. R. DiMaio and J. Ballato, Optics Express **14**, 2380 (2006).
17. R. E. Sherriff and R. P. Devaty, Phys. Rev. B **41**, 1340 (1990); Phys. Rev. B **48**, 1525 (1993); L. M. Claessen, A. G. Jansen, and P. Wyder, Phys. Rev. B **33**, 7947 (1986); G. J. Strijkers, *et al*, IEEE T MAGN **37**, 2067 (2001).